Human Compensation Strategies for Orientation Drifts

Tobias Feigl*
Programming Systems Group
Friedrich-Alexander University
Erlangen-Nürnberg (FAU)

Christopher Mutschler†
Machine Learning and
Information Fusion Group
Fraunhofer IIS

Michael Philippsen
Programming Systems Group
Friedrich-Alexander University
Erlangen-Nürnberg (FAU)

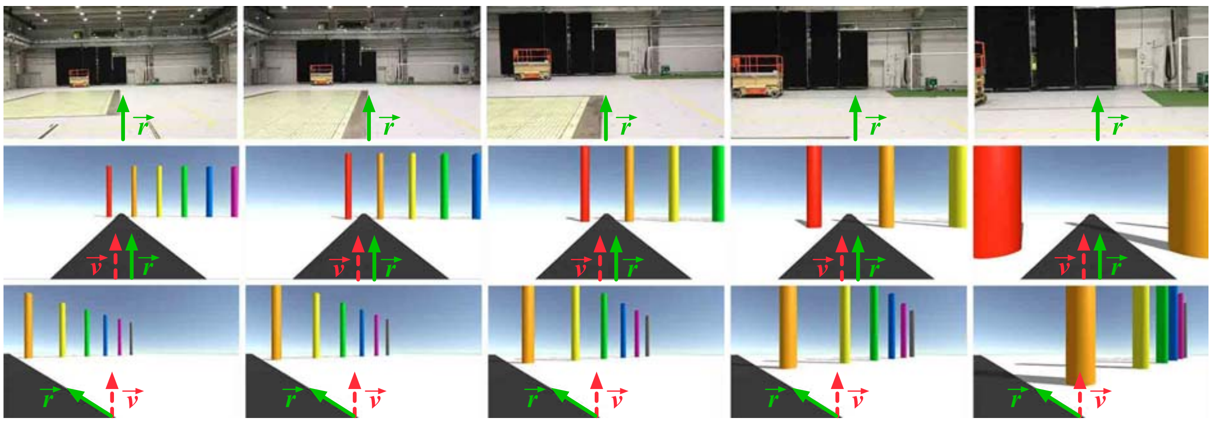

Figure 1: Real (top) and virtual world (mid and bottom row). Real head/view direction $\vec{r}$, virtual view direction $\vec{v}$. Second row: without drift. Bottom row: sensor drift of $45°$ to the right (drift around the vertical body axis, i.e., yaw). Although in the third row the user still looks and walks into the same real view direction $\vec{r}$ as in the top and middle rows, his/her virtual view is drifted by $45°$ to the right. Hence, instead of virtually walking straight ahead towards blue pillar s/he walks sidewards and approaches the orange pillar in the virtual world. The user can either rotate the head by $45°$ or walk sidewards to adjust $\vec{r}$ to $\vec{v}$, or both. If the virtual view $\vec{v}$ diverges from the real view $\vec{r}$, a user is affected by motion sickness that grows with the offset between $\vec{v}$ and $\vec{r}$.

Abstract

No-Pose (NP) tracking systems rely on a single sensor located at the user's head to determine the position of the head. They estimate the head orientation with inertial sensors and analyze the body motion to compensate their drift. However with orientation drift, VR users implicitly lean their heads and bodies sidewards. Hence, to determine the sensor drift and to explicitly adjust the orientation of the VR display there is a need to understand and consider both the user's head and body orientations.

This paper studies the effects of head orientation drift around the yaw axis on the user's absolute head and body orientations when walking naturally in the VR. We study how much drift accumulates over time, how a user experiences and tolerates it, and how a user applies strategies to compensate for larger drifts.

Keywords: VR, orientation drift, head tracking, inertial sensors.

Index Terms: Computing methodologies [Perception] Human-centered computing [Virtual reality]

1 Introduction

VR drives innovation in many applications including theme parks, museums, and simulations. All of them benefit from multi-user interaction and areas beyond 20 $m \times 20$ m. But today's camera-based motion capture systems for such areas can cost 100 $k\$$ or more. Cheaper No-pose (NP) tracking systems only track single positions and can work with such areas, but they cannot be used to derive the pose since their tracking accuracy is insufficient.

The upper row in Fig. 1 shows the view of a user who walks straight ahead with his/her head oriented in the direction of the movement. In the VR (middle row) this movement should lead through the clearance between the red and orange pillars. However, under yaw drift (the bottom row uses a $45°$ heading offset, i.e., a drift of $45°$ around the vertical body axis) the same movement leads to a displacement from right to left as a wrong head orientation $\vec{v}$ is used to render the VR images. For the user the direction of the movement does not fit the VR view.

While today's Simultaneous Localization and Mapping (SLAM)-based inside-out tracking reliably estimates the head's absolute position and orientation in small areas and in lab conditions it fails in large-scale and multi-user environments [8, 9]. Head-Mounted Display (HMD) units are often equipped with inertial measurement units (IMU) such as accelerometers, gyroscopes, and magnetometers that can also be used to estimate the head's pose. But in practice, IMU-based estimations are inaccurate. Both accelerometers (absolute pitch and roll) and gyroscopes (relative pitch, roll, and yaw) cannot estimate the absolute head orientation (w.r.t. yaw). While magnetometers provide absolute yaw orientations they are sensitive to magnetic field variations and often provide a wrong absolute head orientation, e.g., in indoor environments [6]. Dead reckoning based on relative IMU data also leads to drift and thus to a mismatch of the real world and the VR display.

Methods that analyze the IMU signals and determine the sensor drift to compensate for the wrong head orientation [2, 3, 18] also need information on the rotation of the body with respect to the head to perform well. As unfortunately, VR users compensate their movements and their head and body orientations to get along with the drift, there is also a need to consider this compensation.

This paper therefore studies the effect of a drifted VR scene

*Also with Fraunhofer IIS, tobias.feigl@fau.de
†Also with Friedrich-Alexander University Erlangen-Nürnberg (FAU)

2018 IEEE Conference on Virtual Reality and 3D User Interfaces
18-22 March, Reutlingen, Germany
978-1-5386-3365-6/18/$31.00 ©2018 IEEE

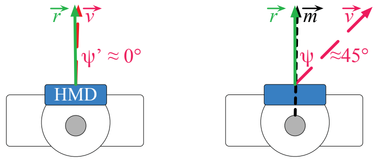

(a) No drift. (b) 45° drift, $\vec{m}{\approx}\vec{r}$.

Figure 2: Two scenarios for a moving user. Offset (yaw drift) ψ between real head direction $\vec{r}$ and virtual head direction $\vec{v}$.

on the head and body orientations of VR users. The knowledge helps large-scale VR-systems, like for example our virtual museum application [13], to handle orientation drift in natural, multi-user applications.

The paper is structured as follows. Section 2 describes the drift situation more formally. Section 3 presents experimental results (on the presence of drift in current state-of-the-art systems and their effects on human perception) and covers types of user strategies to adapt their walks with drifted head orientation. Section 4 reviews the related work.

2 Drift Situation

Relative sensors drift. They inevitably cause a wrong view orientation in the long run. But often there is no choice as absolute sensors (such as magnetometers) are unreliable in practice. (While accelerometers allow for an absolute estimation of pitch and roll, both gyroscopes and accelerometers cannot absolutely estimate the yaw.) Recent SLAM technologies such as Tango [19] (implements a hardware depth sensor with a maximal range of 5 *m*) and ARKit [1] (implements a feature matching algorithm that depends on scene conditions) also do not work since they fail if multiple users occlude the optical sensors or if the tracking area provides little geometrical or textural complexity, e.g., in bad light conditions. As unfortunately, large-scale VR tracking systems avoid physical obstacles to prevent users from collisions their geometrical and textural complexity is too low to provide accurate poses [1, 8, 9, 11, 19].

Fig. 2 illustrates different drift scenarios from a bird's perspective onto a user. The HMD is shown in blue. In Fig. 2(a) there is almost no yaw drift ($\psi{\approx}0°$). As the user's real head orientation $\vec{r}$ is close to his/her virtual head orientation $\vec{v}$, movements feel natural as the correct orientation is used to render the VR image. In Fig. 2(b) a drift of $\psi{\approx}45°$ has accumulated and $\vec{v}$ and $\vec{r}$ differ. When the user moves in the direction of $\vec{m}$ s/he recognizes this offset as an unnatural/wrong translation of the rendered camera image towards $\vec{v}$. Fig. 3 is a zoomed-out representation of this situation with the user at the bottom and the colored pillars from Fig. 1 at the upper end of the grid. The user moves forward in direction $\vec{m}$ in two steps. The user tries to walk towards the blue pillar because the VR display suggests that it is straight ahead. But in reality the user's head/body is oriented in direction $\vec{m}$. What causes motion sickness is that when

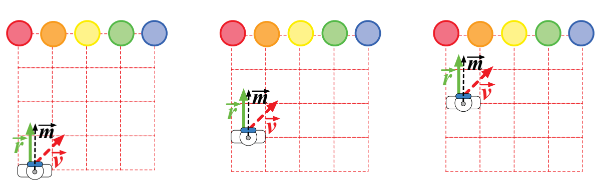

Figure 3: Forward movement $\vec{m}$ that causes virtual sidewards movement due to ψ=45° drift.

the user moves straight ahead in reality (in direction $\vec{m}$) with the intention to reach the blue pillar, the VR view shows a sidewards movement, see also the bottom row of Fig. 1. In the third step of Fig. 3 the user sees the yellow pillar straight ahead in direction $\vec{v}$ as the VR display suffers from the drift.

With a small ψ the user does not feel any inconvenience, see Sections 3 and 4. With a larger ψ the user feels as if s/he is pulled away sidewards while approaching the target because the distortion of relative distances affects every object the user sees in the VR. In reality users compensate for the drift in Fig. 3. To reach the clearance between the red and the orange pillar they usually align $\vec{m}$ closer to $\vec{v}$, i.e., they turn their heads. With larger ψ (see Section 3.3) the users not only align their heads but also their body orientation to align $\vec{m}$ to $\vec{v}$. Methods that consider the IMU signals in combination with the users' movements in VR need to understand the users' compensation strategies as these affect the IMU signals and the users' locomotion.

3 Experiments

Section 3.1 demonstrates that state-of-the-art IMUs accumulate a significant drift within a few minutes. Section 3.2 studies how much drift users tolerate unconsciously. Section 3.3 evaluates the compensation strategies that users apply to deal with larger drifts before Section 3.4 discusses our findings in general.

On a tracking space of about 40 $m \times 35$ m, all our experiments use a Samsung Galaxy Note 4 smartphone (Android 6.0.1, Qualcomm Snapdragon 805 CPU, and 3 *GB* RAM) that has a 6 *DOF* IMU sensor from InvenSense (MPU-6500) attached to a Samsung GearVR HMD (version SM-R320, with a 6 *DOF* Bosch BMI055 IMU sensor), see Fig. 4(a). The HMD in combination with the Unity/Oculus framework provides a relative head orientation at about 60 *Hz* (ORI_{rel}). We record the absolute positions with two different absolute tracking systems. (1) Our radio-frequency NP-tracking system (POS_{abs}) tracks more than 100 users at ≈20 *Hz* on an area up to 100 $m \times 100$ m with a circular error probable 95% of 22.4 *cm* per user [5], see Fig. 4(a). Similar NP-tracking systems are open-source (including hardware) and can be used to reproduce our experiments [17]. (2) An optical NIKON iGPS system (POS^{ref}_{abs}) precisely (<10 *mm*) determines the absolute body pose at ≈30 *Hz*. We use four tracking targets, two of which are mounted on both the head and the shoulders of a user, see Fig. 4(b).

To position the users in the VR we use POS_{abs} and to measure their absolute head/shoulder orientations and their positions we use POS^{ref}_{abs}. We also use POS^{ref}_{abs} as the ground truth and (re)calibrate the relative head orientation of ORI_{rel} for every user and experiment before the user starts walking. While walking we use the relative orientations provided by ORI_{rel} to render the rotation of the VR images.

(a) HMD sensor with relative orientation ORI_{rel} and NP-tracking sensor for absolute position POS_{abs}.

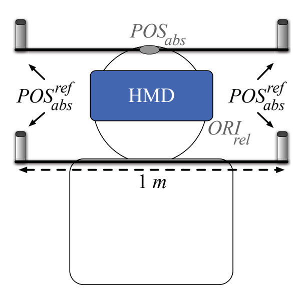

(b) 2·2 iGPS sensors (POS^{ref}_{abs}) to measure the absolute orientation of the head and the body.

Figure 4: Hardware setup used for the experiments.

We determine the *P*oint of *S*ubjective *E*quality (*PSE*) according to [16]. We take the "no orientation drift" state (ORI_{rel}=POS^{ref}_{abs}) as *PSE*=0° at which the subjects perceive the virtual and real movements to be identical. Users notice a (positive or negative) drift as soon as they feel a discrepancy between their virtual and real movements, e.g., when the drift is above $PSE\pm10°$. As users can only tell apart "drift" from "no drift" situations we provide results in the form of $PSE\pm X°$, where X represents the extrema (minimum or maximum) when drift becomes noticeable.

For our studies we had a total of 67 participants. According to the "within-subjects" study design [7], our experiments are independent. We do not compare participants across experiments, but we have overlapping subsets, i.e., some participants performed all experiments (from Section 3.1 to Section 3.3, in this order). We do not design our study according to the "*J*ust *N*oticeable *D*ifference" (*JND*) rule [10], as we need absolute detection thresholds that reliably hold for every VR user (i.e., the threshold based on the most sensitive user).

To measure simulator sickness all subjects answered the Simulator Sickness Questionnaire (*SSQ*) [7] immediately before and after each experiment. Below we use the *SSQ* score notation (N)ausea, (O)culomotor, (D)isorientation, and TS=N+O+D.

Users were only introduced to the study and its risks, but were not aware of the study design and the hypotheses. The real environment was bright and free from acoustical noise. To make users feel more comfortable, the floor of the VR scenes were textured with a checkerboard pattern that is left out from Fig. 5.

3.1 Drift Accumulation Study

To understand the influence of head-to-body motion on the yaw drift we first investigate the sensor drift under rotations *without* sudden and strong changes (i.e., with linear motions only) that are within the range of typical head rotation speeds in VR (synthetic VR movement). Second, we investigate the sensor drift under rotations *with* the sudden and strong speed changes (i.e., with nonlinear motions) of typical head rotations in real VR movement. To evaluate the accumulation of drift over time we start with freshly calibrated HMD motion sensors ($\vec{v}$=$\vec{r}$). The ground truth is POS^{ref}_{abs}. As only the head orientation matters for this experiment, we did not use the shoulder sensors.

Synthetic VR movement. We measure the orientation drift of the Samsung GearVR that sits on a rotary plate (Aerotech ARMS260, with max. 1500 $°/s$ at <0.0007° resolution) and spins for 30 minutes by 32 $°/s$ and for the same time by 41 $°/s$. This is the typical range of head rotation speeds in VR that we found in which 11 subjects (avg. age 28.14 years (min.: 19, max.: 52); avg. height 1.72 m (min.: 1.51, max.: 1.78); without disabilities; all are members of the department (students, engineers, scientist); normal or corrected to normal vision; 4 wear glasses; only 1 had no experience with walking in VR environments; 7 male, 4 female) who walked naturally and relaxed.

For the different synthetic angular rotation speeds, Table 1 shows on its left side that with smooth linear motion low-cost IMU sensors accumulate a drift of 4.4° (= 5 · 0.87°) to 8.6° (= 5 · 1.71°) within 5 minutes. The drift is the difference between the real orientation $\vec{r}$ (from the precise rotary plate system) and the virtual viewing direction $\vec{v}$ (from ORI_{rel}). As we found that drift accumulates almost linearly over time it suffices to measure ψ at the end of the 30 minutes interval.

Real VR movement. In reality the drift is also influenced by different environmental conditions such as the user's activity (e.g., walking, standing, and turning), the user's speed of movement [15], and the user's action (e.g., first-person-shooter gaming versus visiting a virtual museum). We record the drift accumulation in a typical VR experience with 34 participants (avg. age 25.03 years (min.: 16, max.: 48); avg. height 1.74 m (min.: 1.49, max.: 1.81); without disabilities; all are members of the department (students, engineers, scientist); normal or corrected to normal vision; 11 wear contact lenses or glasses; only 2 had no experience with walking in VR environments; 20 male, 14 female). First they walk naturally and relaxed for 10 minutes with an average speed of 0.87 m/s (we ask them to walk at a normal speed; min.: 0.59 m/s, max.: 1.21 m/s, SD: 0.19 m/s) along the zigzag trajectory t that is shown in Fig. 5(a). To see varying head rotation speeds along t, the distance between the horizontal pillars is three times the distance between the vertical pillars (1 m). Second, they walk along t at a fast speed, but still in a natural and relaxed way (avg.: 1.43 m/s, min.: 1.23 m/s, max.: 2.01 m/s, SD: 0.25 m/s) for 10 minutes. Participants always start with a freshly calibrated HMD. We measure the drift $\vec{v}$ as before, again with POS^{ref}_{abs} being the ground truth.

The right hand side of Table 1 shows the average accumulated drift over time for the different movement speeds. Even with a low average speed of 0.87 m/s (and an average angular rotation speed of 32.36°) low-cost IMU sensors accumulate a drift of about 24.7° (= 5 · 4.94°) within 5 minutes. There is even more drift at higher speeds.

Although every participant accelerates her/his head differently, for all of them the accumulated drift is about the same (SD: 0.18° to 0.35°). Hence, showing the averages in Table 1 is sufficient.

Every 60 seconds we asked the users if $\vec{v}$=$\vec{r}$ holds, i.e., if they think that their virtual yaw orientation matches their real yaw orientation. At some point they all perceived a drift. When walking at a normal speed the most sensitive users started to notice a drift at about $PSE\pm19°$. The interval $[PSE\text{-}19°; PSE\text{+}19°]$ holds the imperceptible drifts for all participants. At fast speeds $[PSE\text{-}27°; PSE\text{+}27°]$ remained unnoticed.

No participant verbally reported any symptoms of simulator sickness. The average pre-SSQ score for all subjects is 41.22 (N=2.25, O=4.68, D=4.09) and the post-SSQ score is 43.23 (N=1.96, O=4.68, D=4.91). The individual scores do not vary much. Even for drifts above 27°, TS does not significantly increase within 10 minutes.

We can clearly see that sudden and strong speed changes (i.e., nonlinear motions or real VR movements) in the head-to-body motion result in larger orientation drifts than gradual and small changes (i.e., linear motions or synthetic movements). Now that we know that there is drift (5 times stronger in real than in synthetic move-

Table 1: Rotation speed ω and accumulated drift ψ for both normal and fast synthetic, and normal and fast real movement.

	normal, synthetic	fast, synthetic	normal, real (0.87 m/s)	fast, real (1.43 m/s)
ω [°/s]	32	41	(avg.) 32.36 (min.) 0.05 (max.) 113.69 (SD) 27.91	(avg.) 41.18 (min.) 0.06 (max.) 276.24 (SD) 46.84
ψ [°/min]	0.87 (SD) 0.09	1.71 (SD) 0.15	4.94 (SD) 0.18	5.49 (SD) 0.35

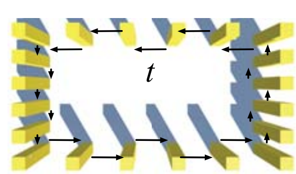

(a) Drift accumulation study: participants walk along the trajectory t at different speeds.

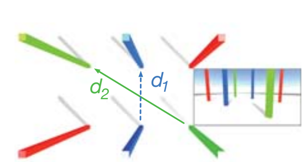

(b) Drift tolerance study: participants walk between blue (d_1=16 m) and green pillars (d_2=32 m).

Figure 5: VR scenes used in the evaluation.

ments) we need to find the threshold above which users notice the drift and compensate for it.

3.2 Drift Tolerance Study

To check whether drift matters, 44 users (avg. age 31.09 years (min.: 18, max.: 60); avg. height 1.77 m (min.: 1.54, max.: 1.94); without disabilities; all are members of the department (students, engineers, scientist); normal or corrected to normal vision; 9 wear contact lenses or glasses; only 3 had no experience with walking in VR environments; 33 male, 11 female) walk through the VR scene shown in Fig. 5(b). They walk two trajectories: the d_1=16 m from one blue pillar to the other and the d_2=32 m from one green pillar to the other. In a natural and relaxed way, they walk each path 5 times in a counterbalanced setup, i.e., half of the users start with d_1, the other half with d_2. While they are on their tracks, we gradually increase the drift of their VR displays by a rate of 1 $°/s$ using linear interpolation around the vertical body axis (yaw) [14]. We ask users to walk naturally, relaxed, and with a normal speed of approximately 1 m/s and to immediately stop as soon as they notice the drift.

The head and body positions and orientations are again recorded with POS_{abs} and POS_{abs}^{ref} while the VR scene is rendered based on positions from POS_{abs} and the calibrated head orientation from ORI_{rel}.

Fig. 6 shows how many participants cover which distances before they notice the drift. For the d_1=16 m walk (avg.: 1.13 m/s, min.: 0.76 m/s, max.: 1.57 m/s, SD: 0.07 m/s) users stop after 10 m to 16 m, i.e., when (depending on a user's actual walking speed) the accumulated drift is between 10° and 17° (avg. 13.03°). For the d_2=32 m walk (avg.: 1.21 m/s, min.: 0.87 m/s, max.: 1.59 m/s, SD: 0.071 m/s) they stop after 20 m to 33 m, i.e., when the drift is between 20° and 33° (avg. 25.97°).

The faster the users approached the target, the less drift their HMD accumulated. The closer the users were to the target, the earlier they noticed even a small drift. Fig. 6 shows the mean (μ) and standard deviation (SD) of the velocities of all users of a bin. While the smallest drifts are noticed by users who walk the fastest and who get closest to the target, large drifts are noticed by users

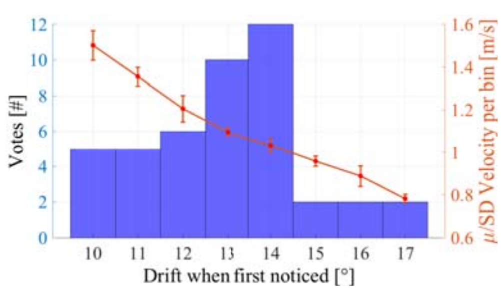

(a) d_1=16 m.

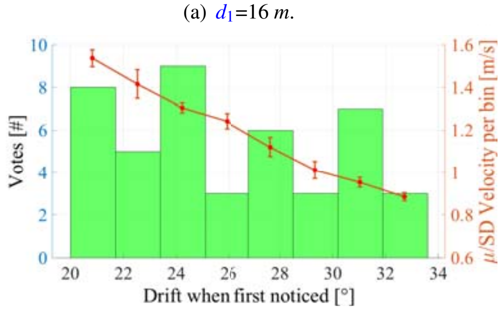

(b) d_2=32 m.

Figure 6: Accumulated drift when users first notice it on the two trajectories: d_1=16 m (top) and d_2=32 m (bottom).

that walk the slowest (i.e., farthest to the target). Two participants noticed the drift only when they already had passed the target pillar. These results match those from similar studies [16]. They show that the perception of drift depends on the objects in the VR. With more and closer objects in the d_1 walk, a small drift of 10° to 17° is already noticeable. In the d_2 walk, users tolerate drifts up to 20°. The closer to the users virtual objects are, the smaller is the drift that they tolerate.

We found that the difference between the perceived virtual and real movement increases with a growing drift and with a shrinking distance to objects. All users noticed changes in the virtual movement, with drifts at $PSE \pm 10°$ (during the d_1 walk at faster movement speeds, up to 1.57 m/s) and $PSE \pm 20°$ (during the d_2 walk at faster movement speeds, up to 1.59 m/s). Thus, the intervals $[PSE\text{-}10°; PSE\text{+}10°]$ and $[PSE\text{-}20°; PSE\text{+}20°]$ represent imperceptible drifts for all participants while walking along d_1 or d_2. We hence suggest a drift tolerance threshold of 10° for a variable user-to-object distance. A drift of 10° is first noticed at a user-to-object distance of 6.9 m while walking with 0.91 m/s along d_1.

Again, no participant verbally reported any symptoms of simulator sickness. The average pre-SSQ score for all subjects is 27.59 (N=1.08, O=3.45, D=2.85) and the post-SSQ score is 34.53 (N=1.30, O=4.13, D=3.80). Here, D grows more than the other scores (post minus pre is 0.95) across all our experiments. But according to the findings in [16] this is not an indicator of simulator sickness. Nevertheless, even for drifts above 20°, TS did not significantly increase over 10 walks.

We achieved the same results when the apparatus of POS_{abs}^{ref} was no longer used (after the initial calibration of ORI_{rel}), so that users could move more freely. By (re)calibrating ORI_{rel} with POS_{abs}^{ref} before/after every single walk we excluded uncontrolled variabilities but also measured the offset, i.e., drift between ORI_{rel} and POS_{abs}^{ref}. The drift/offset during the d_1 walks is smaller than during the d_2 walks. The latter shows drift/offset "observational errors" of 0.54° on average (min: 0.39°, max: 0.62°, SD: 0.07°).

Now we know that users notice orientation drifts above 13° to 25°, depending on their distance to virtual objects. Below we investigate how users adapt their locomotion above these thresholds.

3.3 Drift Compensation Techniques

In all our practical VR work we observed that users compensate a noticed drift by changing their head and body directions and their movements. We identified the following strategies in previous studies and also in the video data that we recorded. Figs. 7(b)-(c) again show the zoomed-out representation known from Fig. 3. As before, the user walks in direction $\vec{m}$ while there is a yaw drift of $\psi \approx 45°$ between $\vec{r}$ and $\vec{v}$. This time we show different user strategies to compensate for the effect of the drift. There are two pure forms: *view* and *movement adaptation*, and a combination of them.

View adaptation. With an unchanged body orientation, a user turns the head $\vec{r}$ by $-\psi$ so that the virtual view is correct and $\vec{m}$ aligns with it. See Fig. 7(a).

Movement adaptation. Conceptually, the user turns the body by $-\psi$ and walks sidewards, so that $\vec{m}$ aligns with the virtual view $\vec{v}$. See Fig. 7(b).

Mixture of view and movement adaptation. In practice, the user often applies a mixture of both strategies. S/he turns both the head $\vec{r}$ and the body against the direction of the drift so that both sum up to $-\psi$, the virtual view is correct, and $\vec{m}$ aligns with it, when the user walks slightly sidewards. See Fig. 7(c).

To prove that there are these compensation strategies, 51 participants (avg. age 27.03 years (min.: 17, max.: 57); avg. height 1.76 m (min.: 1.52, max.: 1.89); without disabilities; all are members of the department (students, engineers, scientist); normal or corrected to normal vision; 12 wear contact lenses or glasses; only 6 had no experience with walking in VR environments; 38 male, 13 female) walk 5 times a straight line (40 m on average) in a simple VR scene (like Fig. 5(b), starting from a common start position). They were asked to walk naturally and relaxed and to somehow get along with drifted visuals in their HMDs.

While a user is on the way we again apply an increasing drift (1 $°/s$) and record the head and body orientation and the position on time-synchronized video and with POS_{abs}^{ref}. From the recordings we semi-automatically determine the drift compensation techniques that the user applies. To analyze the video and all the ORI_{rel} and POS_{abs}^{ref} recordings for changes in the head and body orientation over time, we automatically synchronize the position, the synthetic drift, and head orientation, and then manually synchronize the video stream. As our setup is time synchronized. Drift values can be matched to corresponding head and body orientations in the video, in the ORI_{rel} data, and in the POS_{abs}^{ref} streams. Besides the POS_{abs}^{ref} orientations of the head and shoulders, the video stream also provides the best trade-off to accurately monitor the motion and the synchronized drift over time.

Since for distances above 32 m the participants do not notice any drifts below 15° (the drifts that the most sensible users first noticed were 15.3°, 17.6°, 18.4°, and 24.2°), Table 2 starts from ψ=15° and reports readings in 5° increments. Ignore the Δ-columns for now. While there are users (3, 4, 12, 27, 5) that purely use view adaption, nobody uses movement adaption alone. When users first notice a drift they start to compensate their views (3, 4, 12). There is a steep increase above 20°. For a larger drift they also add movement adaptation. Above 35° about 75 % of the participants (39 of 51) compensate the drift by adapting their view and/or their movement. The sum of view and movement adaptation is always ψ. The Δ-columns represent how many participants have clearly turned their bodies more/less (+/-) between the two given drift values. The larger the drift, the more users add movement adaptation to compensate.

In the videos it is also interesting to note that some participants are unable to walk on a straight line because of the drift. At first, they are pulled sidewards, i.e., their movement direction $\vec{m}$ also adjusts to the drifted VR display. But as soon as they notice the drift, the adaption strategies kick in as described above. Participants that walk at lower speeds (min.: 0.35 m/s; avg.: 0.89 m/s; max.: 1.02 m/s, SD: 0.19 m/s) are affected by larger drifts ($\psi \in [35°; 91°]$). These users then tend to keep (or even relax) the current view adaptation and increase the movement adaptation.

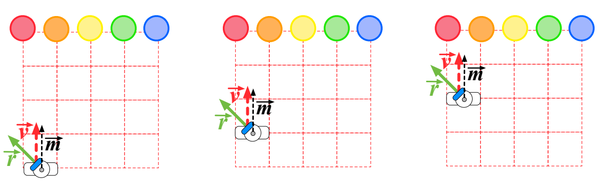

(a) View adaptation: turn head to the left, walk straight.

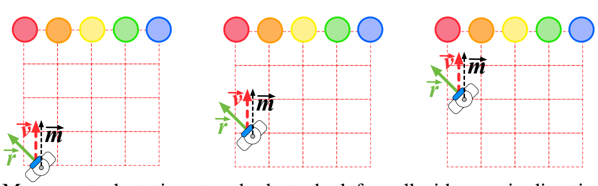

(b) Movement adaptation: turn body to the left, walk sideways in direction $\vec{v}$.

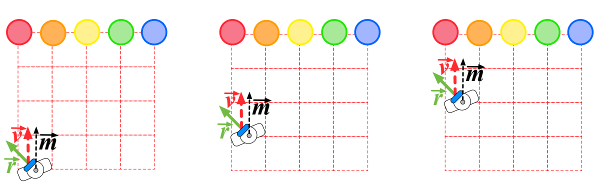

(c) Mixture of (a) and (b): turn head to the left, walk sideways in direction $\vec{v}$.

Figure 7: Human drift compensation strategies.

We also found that the difference between virtual and real movement increases. With a growing drift and with a shrinking distance to objects all users noted that the virtual movement changes, i.e., they started to notice a drift, with drifts above the extrema $PSE \pm 15.3°$. Thus, the interval $[PSE\text{-}15°; PSE\text{+}15°]$ represents imperceptible drifts for all participants when walking naturally.

Again, no participant verbally reported any symptoms of simulator sickness. The average pre-SSQ score for all subjects is 27.65 (N=2.82, O=3.82, D=3.82) and the post-SSQ score is 28.68 (N=1.12, O=3.27, D=3.28). Overall, the individual SSQ scores do not vary much. Even for drifts above 35°, TS does not significantly increase over the 5 walks.

We achieved the same results when the apparatus of POS_{abs}^{ref} was no longer used (after the initial calibration of ORI_{rel}), so that users could move more freely.

As all participants thought that they had walked sidewards (i.e., had ended in a completely different place), they obviously did not notice their compensation strategies but they did notice the drift.

There are two conclusions to draw from these results. First, NP-tracking systems that only use a head mounted IMU and analyze the body motion to compensate the IMU's drift can only adjust the drift of the display as long as users do not notice the drift and do not compensate by re-orienting their heads and bodies. Second, above a threshold of 13°/25° (depending on how close objects are in the VR) unconscious compensation strategies kick in. These can be abused to improve techniques like redirected walking (RDW) and human activity recognition (HAR), and to sustain immersion.

3.4 Discussion

Users noted that they were not afraid to walk, but felt free, natural and relaxed throughout the three studies. We think this is mainly based on the fact that users had seen the large and obstacle-free environment (50 × 50 m) before the studies. This implies that our findings represent natural and "close to reality" results.

While the drift accumulation study compares low-cost head-mounted sensors both in scenarios of linear (machine) and nonlinear (human) motion it also covers typical human motion in VR (e.g., walking at different speeds, running, sidewalks, turns, etc.) and thus represents real world motion scenarios.

The drift tolerance study is in line with our observations from every day use. We do not see differences from real world use cases as our studies are influenced by the knowledge that we have gained from our large scale VR system.

Comparing the PSEs of the studies from Sections 3.1 and 3.2 we state that drift is noticed later if users do not focus on it. In Section 3.1 users do not focus on drift and first notice it at ±19° while in Section 3.2 they already notice it at ±10° at a similar walking speed of 1.5 m/s.

To find tight thresholds we asked the users to really focus on the drift in Section 3.3. Therefore, the study on the drift compensation technique represents every possible human motion. Hence, we now know that if users are moving while paying attention to their head-to-body orientation, we have to keep the yaw orientation drift at least

Table 2: Applied Drift Compensation Strategies.

	15°	20°	$\Delta^{mv}_{20°\to25°}$ +	$\Delta^{mv}_{20°\to25°}$ -	25°	$\Delta^{mv}_{25°\to30°}$ +	$\Delta^{mv}_{25°\to30°}$ -	30°	$\Delta^{mv}_{30°\to35°}$ +	$\Delta^{mv}_{30°\to35°}$ -	35°
Only view	3	4			12			27			5
Mixture	0	0	1	0	2	7	0	7	33	0	34
Only movmt.	0	0			0			0			0

below 20° to ensure that users do not apply a mixed compensation strategy. If users mix the strategies it is almost impossible for today's head-mounted tracking systems to correctly estimate the body pose.

While lower drifts obviously do not lead to motion sickness, we explain the low TS values at drifts above 35° with the fact that users compensate these drifts (e.g., by intuitively applying a mixture of the compensation strategies) to ensure natural movement within an adequate *PSE* interval.

Our findings can help in developing novel motion models for sensor fusion methods to create highly immersive, robust and stable VR tracking systems.

4 Related Work

To the best of our knowledge, there is no publicly available work that considers both the reaction and compensation strategies of humans that freely walk under the influence of heading orientation drift in a large-scale VR tracking system.

All the drift-related research that we know of [4, 12, 14–16] works with much smaller tracking environments. The published experiments only involve much smaller numbers of participants. Or they do not consider a freely walkable VR space but instead apply external or absolute correction systems [3, 19]. And none of the earlier studies works with a No-Pose VR system at all.

Steinecke et al. [16] show that for their environment the perception of drift depends on the closeness of objects that are visible in a user's VR display. We show that also for a more general setting, with closer objects drift is noticed earlier.

There is only little research on user reaction when a drift is noticed [15] (although with freely walking users). The majority of work focuses on manipulating the user by means of a drift that remains unnoticed. Redirected walking (RDW) relies on the availability of accurate pose estimations and artificially includes small drifts into the VR display to modify a user's distance perception and orientation in the VR. Here the idea is that the drift remains unnoticed. Instead of enlarging the available perceived virtual space with RDW and instead of using the full pose we use a large area to investigate the impact of drift on users, especially when there is only NP sensor data available. Our findings are in line with some results from RDW [16]: users do not notice virtual head rotations that are up to 29 % higher or 20 % lower than their real head rotations. Hence, at a normal to fast VR walking speed of 1 m/s a user can be re-oriented without noticing it as long as the drift is below 17° [15].

5 Conclusion

This paper studies the effects of head orientation drift on the users of large scale No-Pose VR systems. The three main findings are: (a) Current low-cost HMD systems accumulate a drift at about 25° or more within 5 minutes of movement. (b) Most users notice such a drift, or even a smaller drift (13°) if the objects in the VR display are close. (c) Most users apply a mixture of view and movement adaptations to compensate drifts above their threshold. The larger the drift is, the more movement adaptation they use. This knowledge is key to sustain immersion and to explorer RDW and HAR ideas for multi-user VR applications. Based on our findings we can now explore and improve human-centric tracking algorithms that take care of the drift, its effects on VR users' motion, and thus provide a more robust and immersive head orientation estimates, and thus a better VR experience.

Acknowledgments

This work was supported by the Bavarian Ministry for Economic Affairs, Infrastructure, Transport and Technology and the Embedded Systems Initiative (ESI).

References

[1] M. Buerli and S. Misslinger. Introducing ARKit - Augmented Reality for iOS. In *Apple Worldwide Developers Conference (WWDC'17)*, pp. 1–187. San Jose, CA, 2017.

[2] G. Donato, V. M. Sequeira, and A. Sadka. Stereoscopic helmet mounted system for real time 3D environment reconstruction and indoor ego-motion estimation. In *Proc. Symp. SPIE Defense and Security*, pp. 1–12. Orlando, FL, 2008.

[3] E. M. Foxlin. Head tracking relative to a moving vehicle or simulator platform using differential inertial sensors. In *Proc. SPIE Intl. Symp. AeroSense*, pp. 133–144. Orlando, FL, 2000.

[4] S. Gradl, B. Eskofier, D. Eskofier, C. Mutschler, and S. Otto. Virtual and augmented reality in sports: an overview and acceptance study. In *Proc. ACM Intl. Joint Conf. Pervasive and Ubiquitous Computing (UbiComp'16)*, pp. 885–888. Heidelberg, Germany, 2016.

[5] T. v. d. Grün, N. Franke, D. Wolf, N. Witt, and A. Eidloth. A real-time tracking system for football match and training analysis. In A. Heuberger, G. Elst, and R. Hanke, eds., *Microelectronic Systems: Circuits, Systems and Applications*, pp. 199–212. Springer, 2011.

[6] J. Haverinen and A. Kemppainen. Global indoor self-localization based on the ambient magnetic field. *Robotics and Autonomous Systems*, 57(10):1028–1035, 2009.

[7] R. S. Kennedy, N. E. Lane, K. S. Berbaum, and M. G. Lilienthal. Simulator sickness questionnaire: An enhanced method for quantifying simulator sickness. *Intl. J. Aviation Psychology*, 3(3):203–220, 1993.

[8] M. Klingensmith, I. Dryanovski, S. Srinivasa, and J. Xiao. Chisel: Real Time Large Scale 3D Reconstruction Onboard a Mobile Device. In *Intl. J. Robotics Research*, pp. 1542–1547. Rome, Italy, 2015.

[9] E. Lachat, H. Macher, T. Landes, and P. Grussenmeyer. Assessment and calibration of a RGB-D camera towards a potential use for close-range 3D modeling. *Remote Sens.*, 1(7):13070–13097, 2015.

[10] R. D. Luce and W. Edwards. The derivation of subjective scales from just noticeable differences. *Psychological Review*, 65(4):222–237, 1958.

[11] P. Meier, S. Himane, S. Misslinger, and B. Blachnitzky. Methods and systems for determining the pose of a camera with respect to at least one object of a real environment, 2015. US Patent App. 14/633,386.

[12] J. D. Moss and E. R. Muth. Characteristics of head-mounted displays and their effects on simulator sickness. *Human Factors: J. Human Factors and Ergonomics Society*, 53(3):308–319, 2011.

[13] D. Roth, C. Kleinbeck, T. Feigl, C. Mutschler, and M.-E. Latoschik. Social Augmentations in Multi-User Virtual Reality: A Virtual Museum Experience. In *Proc. IEEE Intl. Symp. Mixed and Augmented Reality (ISMAR-Adjunct)*, pp. 42–43. Nantes, France, 2017.

[14] K. Shoemake. Animating rotation with quaternion curves. *SIGGRAPH Comput. Graph.*, 19(3):245–254, 1985.

[15] F. Steinicke, G. Bruder, J. Jerald, H. Frenz, and M. Lappe. Analyses of human sensitivity to redirected walking. In *Proc. ACM Symp. Virtual Reality Softw. and Techn.*, pp. 149–156. Bordeaux, France, 2008.

[16] F. Steinicke, G. Bruder, J. Jerald, H. Frenz, and M. Lappe. Estimation of detection thresholds for redirected walking techniques. *IEEE Trans. Visualization and Computer Graphics*, 16(1):17–27, 2010.

[17] J. Tiemann, F. Eckermann, and C. Wietfeld. Atlas - an open-source tdoa-based ultra-wideband localization system. In *Intl. Conf. Indoor Positioning and Indoor Navigation (IPIN)*, pp. 1–6. Alcala de Henares, Spain, 2016.

[18] J. Windau and L. Itti. Walking compass with head-mounted IMU sensor. In *Proc. 2016 IEEE Intl. Conf. Robotics and Automation*, pp. 5542–5547. Stockholm, Sweden, 2016.

[19] W. Winterhalter, F. Fleckenstein, B. Steder, L. Spinello, and W. Burgard. Accurate indoor localization for RGB-D smartphones and tablets given 2D floor plans. In *Proc. IEEE/RSJ Intl. Conf. Intelligent Robots and Systems (IROS)*, pp. 3138–3143. Hamburg, Germany, 2015.